



Faculty of Mechanical Engineering



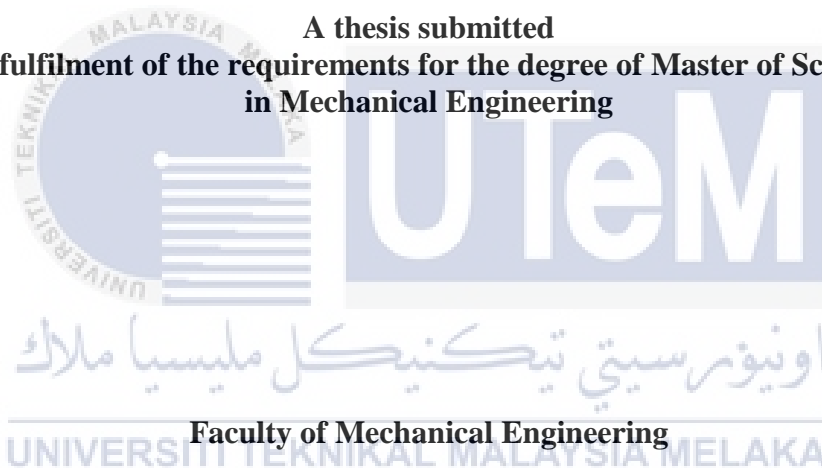
Master of Science in Mechanical Engineering

2020

**INVESTIGATION OF OSCILLATORY-FLOW BEHAVIOUR ACROSS
INTERNAL STRUCTURE IN THERMOACOUSTIC REFRIGERATION SYSTEM**

DAHLIA BINTI JOHARI

**A thesis submitted
in fulfilment of the requirements for the degree of Master of Science
in Mechanical Engineering**



UNIVERSITI TEKNIKAL MALAYSIA MELAKA

2020

DECLARATION

I declare that this thesis entitled “Investigation of Oscillatory-Flow Behaviour Across Internal Structure in Thermoacoustic Refrigeration System” is the result of my own research except as cited in the references. The thesis has not been accepted for any degree and is not concurrently submitted in candidature of any other degree.



Signature :

Name : Dahlia Binti Johari
اونيورسي تيكنيكل مليسيا ملاك

Date :

UNIVERSITI TEKNIKAL MALAYSIA MELAKA

APPROVAL

I hereby declare that I have read this thesis and in my opinion this thesis is sufficient in terms of scope and quality for the award of Master of Science in Mechanical Engineering.

Signature	:
Supervisor Name	:	Dr Ernie Binti Mat Tokit
Date	:

اونيورسيتي تيكنيكل مليسيا ملاك

UNIVERSITI TEKNIKAL MALAYSIA MELAKA

DEDICATION

In honour of my loving parents and siblings



ABSTRACT

Thermoacoustic technology has been recognised as the one of green technology as it provides alternatives green working mechanism for engine and refrigeration system. This is due to its simplicity (as there was no moving parts) and the system also use a non-polluting gas. Unfortunately, the fluid dynamics of the system is complex and not well understood. The fluid that flows inside the system is flowing in oscillatory conditions following the acoustic wave. In this study, flow distribution inside a standing wave thermoacoustic condition is tested experimentally and numerically. The thermoacoustic system is first modelled using DeltaE software. The model is used as benchmark for setting up of a thermoacoustic rig that is suitable for the investigation of the oscillatory flow behaviour across the internal structures in the thermoacoustic system. The components of the rig include the loudspeaker as the acoustic driver, a resonator made of steel and a structure known as a stack made of aluminium. The stack was a parallel-plate structure where most thermoacoustic effects take place. The test rig was build based on a quarter wavelength standing-wave thermoacoustic design. Therefore, for the purpose of investigating the fluid dynamics of oscillatory flow at different frequencies, the resonator was divided into several segments which was assembled according to flow frequency. Due to the complication of design, the study of flow frequencies was limited to only two flow frequencies, which were 14.2 Hz and 23.6 Hz. For 14.2 Hz flow frequencies, the stack was located at two different locations of 0.11λ and 0.18λ from the pressure antinode while 23.6 Hz flow frequencies, the stack was located at 0.18λ from the pressure antinode. The stack was fabricated with two different lengths of 70 mm and 200 mm. The experimental rig was first tested for resonance frequency and references point followed by the investigation of the change of velocity in each point along the thermoacoustic rig as drive ratio (ratio of pressure at antinode to the mean pressure) changes. The DeltaE software models provide pressure distribution data that are similar to the theoretical data and stack with the length of 200 mm gives a better performance in term of drive ratio (Dr) where an increment of drive ratio percentage of 28% was recorded compared to 25% drive ratio increment for the 70 mm stack. Comparisons were also made for first-order harmonic velocity amplitude, u_1 , obtained from three different methods; theoretical calculations, DeltaE software, and the experimentally measured values. It is found that the velocity distribution of flow across the 70 mm long stack results in highest Stoke's Reynolds number which is 271.99 that leads to early starts of turbulence in the flow. The stack's location of 0.11λ was also found to be the best location based on velocity data of the current flow conditions. Besides that, it is also found that 23.6 Hz flow frequency result in the better drive ratio compared to 14.2 Hz. The findings help to understand possible differences between theoretical and real experimental values so that better improvements can be made in the future design of the thermoacoustic system.

ABSTRAK

Sistem termoakustik telah diiktiraf sebagai sistem teknologi hijau yang menyediakan alternatif mekanisma kerja untuk enjin dan sistem penyejukan. Ini kerana keringkasannya (tiada bahagian bergerak) dan menggunakan gas bukan pencemar. Malangnya, sistem dinamik bendalir adalah kompleks dan masih belum difahami dengan baik. Cecair yang mengalir di dalam sistem ini adalah dalam keadaan berayun mengikut gelombang akustik. Dalam penyiasatan ini, pengagihan aliran dalam keadaan gelombang termoakustik berdiri diuji secara eksperimen dan berangka. Sistem termoakustik ini dimodelkan menggunakan perisian DeltaE. Model ini digunakan sebagai penanda aras untuk membina rig eksperimen thermoakustik yang sesuai dalam menyiasat kelakuan aliran berayun disepanjang struktur dalam sistem termoakustik. Komponennya adalah pembesar suara sebagai pemacu akustik, sebuah 'resonator' yang diperbuat daripada keluli dan satu struktur yang dikenali sebagai timbunan yang diperbuat daripada aluminium. Timbunan ini adalah struktur plat selari di mana kebanyakan kesan-kesan termoakustik berlaku. Rig ini dibina mengikut reka bentuk suku gelombang termoakustik berdiri. Maka, untuk menyiasat sistem dinamik bendalir aliran berayun, 'resonator' telah dibahagikan kepada beberapa segmen yang disusun mengikut kepanjangan frekuensi aliran. Disebabkan komplikasi reka bentuk, penyiasatan frekuensi aliran hanya terhad kepada dua frekuensi aliran iaitu 14.2 Hz dan 23.6 Hz. Bagi 14.2 Hz frekuensi aliran, timbunan telah diletakkan di dua bahagian berlainan iaitu 0.11λ dan 0.18λ dari antinod tekanan manakala bagi 23.6 Hz frekuensi aliran, timbunan diletakkan pada 0.18λ dari antinod tekanan. Timbunan dibina dengan dua kepanjangan berbeza iaitu 70 mm dan 200 mm. Rig eksperimen awalnya diuji dengan frekuensi resonan dan titik rujukan diikuti penyiasatan perubahan halaju di setiap titik di sepanjang rig termoakustik sebagai nisbah pemacu (nisbah tekanan pada antinod kepada tekanan purata). Model perisian DeltaE mengeluarkan data tekanan pengedaran yang serupa dengan data teori dan timbunan dengan kepanjangan 200 mm memberikan prestasi lebih baik dengan kenaikan 28% nisbah tekanan berbanding timbunan panjang 70 mm yang hanya mencatatkan kenaikan 25% nisbah tekanan. Perbandingan dari segi amplitud halaju harmonic pertama, u_1 , telah diperolehi dari tiga kaedah berbeza iaitu pengiraan teori, perisian DeltaE dan eksperimen. Halaju pengagihan aliran melalui timbunan 70 mm telah dikenalpasti menghasilkan nombor 'Stoke's Reynolds' yang lebih tinggi dan juga membawa kepada pergolakan awal dalam aliran. Lokasi timbunan pada 0.17λ dari antinod tekanan juga dikenalpasti merupakan lokasi terbaik berdasarkan data halaju pada aliran semasa. Selain itu, aliran frekuensi 23.6 Hz didapati mempunyai nisbah pemacu yang lebih baik berbanding 14.2 Hz. Dapatan kajian ini membantu dalam memahami kemungkinan perbezaan antara nilai teori dan eksperimen bagi penambahbaikan reka bentuk sistem termoakustik akan datang.

ACKNOWLEDGEMENTS

Advertently, I would like to express my sincerest gratitude to those whom are involved in the completion of this thesis, especially to my supervisor Dr Ernie binti Mat Tokit and Dr Fatimah Al-Zahrah binti Mohd Sa'at from the Faculty of Mechanical Engineering Universiti Teknikal Malaysia Melaka (UTeM) who have directly gave guidance as well as teaching me the value of being highly independent. Additionally, I would also keen on extending my deepest gratitude to those involved in the technical aspects of the research, in particular towards all the assistant engineer, Mr Faizal bin Jaafar (Turbo Machinery Lab), Mr Hairul Nezam bin Wahid (Prototype & Innovation Lab), Mr Mohd Yuszrin bin Md Yacob (Fabrication Workshop), Mr Ikhmal Hisham bin Ibrahim (Mechanics of Fluid Lab), Mr Mazlan bin Tumin (Machine Workshop), Mr Asjufri bin Muhajir (Air conditioning Lab), Mr Habirafidi bin Ramly (Control & Vehicle Electronic System Lab), Mr Nor Izwan bin Junoh (Engine Performance Testing Lab) and Mr Mohd Kamil Anuar bin Akram @ Jummah (IDP Workshop) for their assistance, time spent and effort in all the lab works that have been done.

True acknowledgements are dedicated to my loving parents and siblings for the continuous support morally. Lastly, special thanks to my colleague, Siti Hajar Adni Binti Mustaffa for being the best partner in completing our master study together.

TABLE OF CONTENTS

	PAGE
DECLARATION	
APPROVAL	
DEDICATION	
ABSTRACT	i
ABSTRAK	ii
ACKNOWLEDGEMENTS	iii
TABLE OF CONTENTS	iv
LIST OF TABLES	viii
LIST OF FIGURES	x
LIST OF APPENDICES	xv
LIST OF SYMBOLS	xvi
LIST OF PUBLICATIONS	xvii
CHAPTER	
1. INTRODUCTION	1
1.1 Research background	1
1.2 Problem statement	3
1.3 Objectives	4
1.4 Significance of the project	5
1.5 Scope of the project	5
1.6 Thesis outline	
2. LITERATURE REVIEW	7
2.1 Overview	7
2.2 Historical background on thermoacoustic research	7
2.2.1 Performance parameter in the thermoacoustic system	11
2.2.1.1 Wavelength, λ and frequency, f	12
2.2.1.2 Amplitude of gas displacement	13
2.2.1.3 Thermal penetrations depth δ_k , and viscous penetration depth δ_v	15
2.2.1.4 Prandtl number	16
2.2.1.5 Porosity and hydraulic radius	17
2.2.1.6 Drive ratio	18
2.3 Thermoacoustic principles	18
2.3.1 Standing waves engine	20
2.3.2 Standing waves refrigerator	23

2.3.3	Travelling waves engine and refrigerator	24
2.4	Design parameters of the thermoacoustic system	26
2.4.1	Working fluid	26
2.4.2	Resonance frequency	27
2.4.3	Resonator	28
	2.4.3.1 Resonator material	29
	2.4.3.2 Resonator geometry	30
2.4.4	Stack	32
	2.4.4.1 Stack's material	33
	2.4.4.2 Stack's location	34
2.5	Oscillatory flows	35
2.6	DeltaE software	38
2.7	The current study in the context of the existing literature	39
2.8	Summary	40
3.	METHODOLOGY	41
3.1	Overview	41
3.2	Design of experiment by Using DeltaE software	43
3.2.1	Zeroth segment (BEGIN)	47
3.2.2	First segment (VSpeaker)	48
3.2.3	Short duct (loudspeaker box)	49
3.2.4	Conical section	49
3.2.5	Minor	50
3.2.6	Duct	51
3.2.7	Stack	51
3.2.8	Hardend	52
3.2.9	The schematic diagram for each case in the DeltaE software	52
3.3	Experimental design	53
3.3.1	Resonator's design	54
	3.3.1.1 Resonator material	55
	3.3.1.2 The calculation of the resonator length	56
3.3.2	Stack's design	57
	3.3.2.1 Stack's material	57
	3.3.2.2 Location of stack	58
	3.3.2.3 Dimension of stack	60
3.3.3	The fabrication of loudspeaker box and contraction parts	61
3.3.4	Fabrication of the lid of the test section	64
3.4	Experimental equipment and sensor	65
3.4.1	Measuring equipment	66
3.4.2	Connection of the instrument and sensors	67
3.5	Experimental debugging	70

	3.5.1	Resonance frequency	71
	3.5.2	Stability of the measurement data	71
	3.5.3	References point	71
3.6		Measurement of pressure and velocity	73
	3.6.1	Measurement of 14.2 Hz rig (6.6-meter resonator)	73
	3.6.2	Measurement of 23.6 Hz rig (3.8-meter resonator)	75
3.7		Summary	76
4.		RESULT AND DISCUSSION	77
4.1		Overview	77
4.2		DeltaE software prediction data	77
	4.2.1	Resonator with 14.2 Hz frequency	78
		4.2.1.1 Flow distribution inside the resonator (14.2 Hz)	79
		4.2.1.2 Effects of stack's location (14.2 Hz)	80
		4.2.1.3 Effects of stack's length (14.2 Hz)	83
	4.2.2	Resonator with 23.6 Hz frequency	86
	4.2.3	Effects of operating frequency between 14.2 Hz and 23.6 Hz	88
4.3		Experimental debugging	90
	4.3.1	Measured resonance frequency through experimental work	91
		4.3.1.1 The 6.6 m length resonator	91
		4.3.1.2 The 3.8 m length resonator	93
	4.3.2	References point of flow amplitude	94
		4.3.2.1 References point for the resonator with 14.2 Hz frequency	94
		4.3.2.2 References point for the resonator with 23.6 Hz frequency	97
4.4		Comparison of DeltaE software, theoretical value and experimental result	100
	4.4.1	Effects of stacks length	100
	4.4.2	Effects of stacks location	105
	4.4.3	Effects of frequency	108
	4.4.4	The percentage difference between the theoretical calculation and the measured experimental data	111
4.5		Summary	113

5. CONCLUSION AND RECOMMENDATION	114
5.1 Conclusion	114
5.1.1 Objective 1	114
5.1.2 Objective 2	115
5.1.3 Objective 3	115
5.2 Recommendation	116
REFERENCES	118
APPENDICES	132



LIST OF TABLES

TABLE	TITLE	PAGE
2.1	Properties of air (Munson et al., 2013)	27
2.2	Properties of different stack materials	34
3.1	The parameter for the begin segment	48
3.2	The parameter for the Vspeaker segment	48
3.3	The parameter for the short duct segment	49
3.4	The parameter for the conical section segment	50
3.5	The parameter for the minor segment	50
3.6	The parameter for the duct segment	51
3.7	The parameter for the stack segment	51
3.8	Table of cases that are used in this study	53
3.9	Actual operating frequency for the test rig	60
4.1	Summary of the parametric study in the thermoacoustic model for 14.2 Hz frequency	78
4.2	Calculated drive ratio from each of the different parametric cases in DeltaE software	85
4.3	Summary of the cases in the thermoacoustic model for 23.6 Hz	87

4.4	The reference values of velocity and the corresponding drive ratio for the 14.2 Hz frequency resonator with the calculated Stoke's Reynolds Number	95
4.5	Trendline linear equation for 14.2 Hz frequency cases	97
4.6	The reference values of velocity and the corresponding drive ratio for the 23.6 Hz frequency resonator with the calculated Stoke's Reynolds Number	98
4.7	Trendline linear equation for 23.6 Hz frequency cases	99
4.8	The percentage difference for the experimental, theoretical value and DeltaE software results	112



LIST OF FIGURES

FIGURE	TITLE	PAGE
1.1	The thermoacoustic refrigerator sketch. (Marx et al., 2006)	3
2.1	(a) The singing flames (Putnam and Dennis, 1956), (b) Sondhauss Tube, and (c) Rijke tube (Feldman, 1968)	10
2.2	The chronological order of the thermoacoustic history	11
2.3	The illustration of the wavelength	12
2.4	The heat transfer process for the different length of the heat exchangers (Saechan, 2014)	14
2.5	The critical performance parameter in the thermoacoustic device (Shi, 2010)	16
2.6	The relationship between pressure and velocity in (a) a standing wave thermoacoustic device and (b) travelling wave thermoacoustic device (Mohd Saat, 2013)	19
2.7	The schematic diagram of a simple thermoacoustic system. (Marx et al., 2006)	20
2.8	Schematic diagram of (a) standing waves thermoacoustic engine (b) the profiles of pressure and velocity along the resonator (Mao, 2011) (c) temperature profile and the temperature of the gas particle in the thermodynamic cycle along the stack (d) p - V diagram.	22

2.9	Schematic diagram of a standing waves thermoacoustic refrigerator (b) the profiles of pressure and velocity along the resonator (Mao, 2011) (c) temperature profile and the temperature of the gas particle in the thermodynamic cycle along with the stack (d) p - V diagram	24
2.10	Resonator types; (a) half wavelength resonator; (b) quarter wavelength resonator	31
2.11	Resonator optimized for minimized losses per unit area	32
3.1	Flow chart through the research study	42
3.2	The block diagram of the segment in DeltaE software (a) with the stack (b) without the stack	46
3.3	The variables that are being used in the DeltaE software	47
3.4	The schematic diagram for 14.2 Hz rig (a) 200 mm stack location 0.18λ from the antinode (Case 1) (b) 70 mm stack location 0.18λ from the antinode (Case 3) (c) 200 mm stack location 0.11λ from the antinode (Case 2) (d) 70 mm stack location 0.11λ from the antinode (Case 4)	52
3.5	The schematic diagram for 23.6 Hz (a) 200 mm stack location 0.11λ from the antinode (Case 5) (b) 70 mm stack location 0.18λ from the antinode (Case 6)	53
3.6	Schematic diagram for the resonator (a) 14.2 Hz frequency and (b) 23.6 Hz frequency	55
3.7	The mild steel resonator that is built-in compartments	56

3.8	The aluminium stack with 3mm thickness and 6 mm gap in between (a)200 mm length and (b) 70mm length	57
3.9	Schematic diagram for the location of the stack using fundamental frequency 14.2 Hz with the location of (a) 0.18λ from the pressure antinode (b) 0.11λ from the pressure antinode	58
3.10	Schematic diagram for the location of the stack using an operating frequency of 23.1 Hz for 0.18λ	59
3.11	Plasma cutter machine	61
3.12	Schematic diagram of the loudspeaker box	62
3.13	Dimension of the contraction part (a) and (b)	63
3.14	Actual view of the loudspeaker box and contraction part	64
3.15	(a) Acrylic cutting by using a mitre saw (b) Milling process by using a milling machine	65
3.16	(a) Lid for the test section (200mm stack) with the hole at the side (b) the fitted resonator lid to the test section	65
3.17	The sequence of connection to control the excitation of the loudspeaker	68
3.18	(a) BNC cable that connects from 50Ω output from the function generator. (b) the connectors from the BNC cable to the VXML connectors. (c) VXML connectors that connect the connectors of BNC to the XLR panel mounting	68
3.19	Complete set of connection from the function generator to the loudspeaker	69

3.20	Positive Negative cable connects to the loudspeaker from the amplifier XLR connector	69
3.21	The data logger and voltage regulator with the pressure sensor connection	70
3.22	Pressure sensor at the antinode to calculate the drive ratio	73
3.23	Schematic diagram for the location of the sensor for the stack location for 14.2 Hz (a) 0.18λ from the antinode (b) 0.11λ from the antinode	74
3.24	The pressure sensor and the hot wire is attached together to find the velocity and the pressure at each point	75
3.25	Schematic diagram for the location of the sensor for the stack location of 0.18λ from the antinode	76
4.1	Segments for the cases of 14.2 Hz in DeltaE software	78
4.2	The comparison of the pressure behaviour for cases with and without stack (200 mm stack with 14.2 Hz frequency)	80
4.3	(a) 200 mm stack with 0.18λ and 0.11λ from the antinode (b) 70 mm stack with 0.18λ and 0.11λ from the antinode	82
4.4	(a) 200 mm and 70 mm stack with 0.18λ from the antinode (b) 200 mm and 70 mm stack with 0.11λ from the antinode	84
4.5	Segments for the cases of 23.6 Hz in DeltaE software at the stack location of 0.18λ from the antinode	86
4.6	0.18λ from the antinode for 200 mm stack and 70 mm stack	87
4.7	Comparison of the different frequency of the resonator	90

4.8	Setting frequency versus measured drive ratio (6.6 meter resonator)	92
4.9	Setting frequency versus measured drive ratio (3.8 meter resonator)	93
4.10	References point for 0.18λ from the antinode (14.2 Hz)	96
4.11	References point for 0.18λ from the antinode (23.6 Hz)	99
4.12	Comparison of velocity at various drive ratio along the resonator for 200 mm stack at 0.18λ from the antinode (a) the experimental data (b) the theoretical data and (c) the prediction data from DeltaE software	102
4.13	Comparison of velocity at various drive ratio along the resonator 70mm stack at 0.18λ from the antinode (a) the experimental data (b) the theoretical data and (c) the prediction data from DeltaE software	104
4.14	Graph of experimental velocity data of 200 mm stack of the different location at (a) Point A (b) Point B (c) Point C and (d) Point D	106
4.15	Comparison between experimental and DeltaE software velocity data of 70 mm stack of the different locations at (a) Point A (b)Point B (c) Point C and (d) Point D	107
4.16	200 mm stack at a different frequency with (a) experimental data (b) theoretical calculation and (c) DeltaE software prediction	109
4.17	70 mm stack at a different frequency with (a) experimental data (b) theoretical calculation and (c) DeltaE software prediction	110

LIST OF APPENDICES

APPENDIX	TITLE	PAGE
A	The AUTOCAD drawing for the experimental rig	132
B	The equipment and sensors with all the specification	141



LIST OF SYMBOLS

a	-	Speed of sound
C	-	Specific heat capacity
c	-	Speed of light
c_p	-	Isobaric specific heat per unit mass
Dr	-	Drive ratio
f	-	Frequency
K	-	Thermal conductivity
l	-	Length
M	-	Metre
mm	-	Millimetre
P_m	-	Mean pressure
P_a	-	Pressure at antinode
R	-	Gas constant
Re	-	Reynolds number
T	-	Temperature
u_1	-	First order harmonic velocity amplitude
V	-	Volts
\dot{W}	-	Acoustic work
x_s	-	Distance between the pressure antinode of the resonator to the centre of the stack
x_o	-	Centre of the stack
y_o	-	Half of plate spacing
γ	-	Ratio of specific heat capacities
λ	-	Wavelength
ω	-	Angular velocity
δ	-	Ratio of velocity amplitude and angular frequency
ξ	-	Gas displacement
δ_k	-	Thermal penetration depth
δ_v	-	Viscous penetration depth
κ	-	The diffusivity of the gas
ρ	-	Mean density of the gas
μ	-	Dynamic viscosities
ν	-	kinematic viscosities
σ	-	Prandtl number
ϕ	-	Porosity
γ_h	-	Hydraulic radius
ϵ_s	-	Heat capacity ratio

LIST OF PUBLICATIONS

Johari, D., Mat Tokit, E., and Mohd Saat, F.A.Z., 2019. *DeltaE Prediction of Pressure Along a Quarter-Wave Thermoacoustic Test Rig*. Proceedings of Mechanical Engineering Research Day, pp.1-2.

Mohd Saat, F.A.Z., Johari, D., and Mat Tokit, E., 2019. *Experimental Test of a Standing-Wave Thermoacoustic rig*. Proceedings of Mechanical Engineering research Day, pp.1-2.

Mohd Saat, F.A.Z., Johari, D., and Mat Tokit, E., 2019. *DeltaE Modelling and Experimental Study of a Standing Wave Thermoacoustic Test Rig*. International Journal of Mechanical and Production Engineering Research and Development (IJMPERD), (accepted for publication).

Johari, D., Mat Tokit, E., and Mohd Saat, F.A.Z., 2018. *Parametric Study of Thermoacoustic System using DeltaE*. Journal of Advanced Research in Fluid Mechanics and Thermal Sciences, 1 (1), pp. 161–168.

Johari, D., Mat Tokit, E., and Mohd Saat, F.A.Z. 2016. *Instrumentation for Studying the Turbulence Characteristic in Oscillatory Flow Used in Thermoacoustic: A Review*. Postgraduates Symposium for Environment Engineering Technology.

CHAPTER 1

INTRODUCTION

1.1 Research background

Generally, thermoacoustic technology is based on the system of ‘thermoacoustic effect’ and can be divided into two systems, which are refrigerator and heat engine. It is a system that uses acoustic energy and thermal energy conversion without any moving parts in the system, which using non-polluting gases such as helium, argon, xenon, or also known as inert gases. The thermoacoustic technology encompasses the fields of thermodynamics and acoustics as it consumes a little energy input besides the minimum range of fabrication cost. This technology has been very compromising in developing green technology that is advancing rapidly day by day.

Nowadays, green technologies are being developed continuously around the world as the greenhouse effects and climate change is very alarming. This is due to the usage of chemicals that is increasing uncontrollably, such as Chlorofluorocarbon (CFC) that is being used in the cooling system. Scientists and researchers all around the globe are intensely finding new technology and innovation to solve this problem. However, green technologies come with some significant issues such as a very high cost to comply with the existing technology.

Chlorofluorocarbon (CFC) is a stable compound that had been the most common chemical used in many applications such as refrigerant, solvent, synthesis of the plastic and also for many other applications. Even though it has been used in many forms, it is a compound that is non-flammable, tasteless, odorless and not easily being decomposed which

causes a negative effect on the environment and depletion of the ozone layer due to its physical characteristic and heat resistance. Due to this effect, it has been banned from some of the countries to protect the environment. As the effect of the prohibited of the CFC, many researchers give a particular interest in developing green technology to replace the current use of CFC. Thermoacoustic refrigerator and engine are one of the alternatives that have been developed with no refrigerant at all but still in the early investigation due to the unclear effects and its performances.

Back in the 19th century, Rayleigh started the theoretical basis of the acoustic field. In the thermoacoustic system, the exchanging of gas-particle from cold to the hot reservoir was set at the place where there is a supply of acoustic energy at the region of a solid boundary by using a stack, which is in the form of porous shape or parallel plates. The expansion and contraction of the gas particles together with their oscillatory movement allow energy transport and creates a temperature gradient. At an optimum pressure within a closed system, the oscillation of the fluid particles provided a significant temperature gradient as it passes through the stack (Swift, 2001).

The thermoacoustic system is a simple system that only requires a driver or loudspeaker, a resonator and a stack. It requires no moving parts and can be obtained at a reasonable price with no refrigerant needed (Adeff and Hofler, 2000). Figure 1.1 shows the loudspeaker or transducer in the thermoacoustic engine, which is used to provide the acoustic power to the thermoacoustic system. The energy is then converted to the heat flux by the stack. This phenomenon is known as the thermoacoustic effect. A cold heat, Q_c is pumped from the cold reservoir to be cooled down by the cold heat exchanger. As for the hot heat, Q_h is released at the hot heat exchanger and therefore creating the temperature difference. (Marx et al., 2006).